

1 **A Cytosolic Reductase Pathway is Required for Complete N-Glycosylation of an**  
2 **STT3B-Dependent Acceptor Site.**

3 Marcel van Lith<sup>1</sup>, Marie Anne Pringle<sup>1</sup>, Bethany Fleming<sup>1</sup>, Giorgia Gaeta<sup>1,3</sup>, Jisu Im<sup>1,2</sup>, Reid Gilmore<sup>4</sup>,  
4 Neil J Bulleid<sup>1\*</sup>

5 1. Institute of Molecular, Cell and Systems Biology, College of Medical Veterinary and Life Sciences,  
6 Davidson Building, University of Glasgow, Glasgow, G12 8QQ, UK.

7 2. Cellular Protein Chemistry, Faculty of Science, Utrecht University, 3584 CH Utrecht, The  
8 Netherlands

9 3. Nuffield Dept. of Orthopaedics, Rheumatology and Musculoskeletal Sciences, Botnar Research  
10 Centre, Headington, Oxford OX3 7LD. UK

11 4. Department of Biochemistry and Molecular Pharmacology, University of Massachusetts Medical  
12 School, Worcester, MA 01605, USA.

13 ORCID:, MvL (0000-0003-0225-5501), MAP (0000-0002-1358-4610), BF (0000-0002-9774-1256),  
14 GG (0000-0001-7500-9091), JI (0000-0003-0972-3048), RG (0000-0002-1656-4041), NJB (0000-  
15 0002-9839-5279)

16 \* To whom correspondence should be addressed: Tel: +44 141 330 3870, e-mail:

17 [neil.bulleid@glasgow.ac.uk](mailto:neil.bulleid@glasgow.ac.uk)

18 Running title: Redox control of N-glycosylation.

19 **Abstract**

20 N-linked glycosylation of proteins entering the secretory pathway is an essential post-translational  
21 modification required for protein stability and function. Previously, it has been shown that there is a  
22 temporal relationship between protein folding and glycosylation, which influences the occupancy of  
23 specific glycosylation sites. Here we use an *in vitro* translation system that reproduces the initial  
24 stages of secretory protein translocation, folding and glycosylation under defined redox conditions.  
25 We found that the efficiency of glycosylation of hemopexin was dependent upon a robust NADPH-  
26 dependent cytosolic reductive pathway, which could also be mimicked by the addition of a membrane  
27 impermeable reducing agent. The identified hypoglycosylated acceptor site is adjacent to a cysteine  
28 involved in a short range disulfide bond, which has been shown to be dependent on the STT3B-  
29 containing oligosaccharyl transferase. We also show that efficient glycosylation at this site is  
30 dependent on the STT3A-containing oligosaccharide transferase. Our results provide further insight  
31 into the important role of the ER redox conditions in glycosylation site occupancy and demonstrate a  
32 link between redox conditions in the cytosol and glycosylation efficiency.

### 33 **Introduction**

34 Proteins entering the secretory pathway are subject to a variety of modifications, the most prevalent of  
35 which include N-linked glycosylation and disulfide formation (Bulleid, 2012; Cherepanova et al.,  
36 2016). N-glycosylation is catalysed by one of two oligosaccharyl transferases (OST) that transfer a  
37 pre-formed oligosaccharide from a dolichol-phosphate intermediate to asparagine residues on the  
38 polypeptide chain within the consensus sequence -N-X-S/T where X is any amino acid other than  
39 proline (Kelleher et al., 2003). The two OST isoforms are multi-subunit complexes characterised by  
40 the catalytic subunits STT3A or STT3B with common subunits as well as complex-specific subunits  
41 including DC2 and KCP2 for the STT3A, and the thioredoxin-domain containing proteins MagT1 or  
42 TUSC3 for the STT3B complex (Blomen et al., 2015; Roboti and High, 2012; Shibatani et al., 2005).  
43 It has been demonstrated previously that the STT3A complex associates with the ER translocon  
44 (Braunger et al., 2018; Shibatani et al., 2005) and catalyses the co-translational glycosylation of  
45 proteins, whereas the STT3B complex glycosylates sites skipped by STT3A acting predominantly  
46 post-translationally (Cherepanova et al., 2014; Ruiz-Canada et al., 2009). Because of their distinct  
47 specificities, some substrates require the STT3A or STT3B complexes for efficient glycosylation  
48 (Cherepanova and Gilmore, 2016; Cherepanova et al., 2014). Indeed, recent proteomic analysis of  
49 glycoproteins synthesised in either STT3A or STT3B depleted cells identify classes of STT3A and  
50 STT3B dependent N-glycosylation sites (Cherepanova et al., 2019). Deficiency of the STT3B  
51 complex cannot be compensated by the STT3A complex, resulting in hypoglycosylation of substrates  
52 affecting their function and leading to disease pathologies linked to immunodeficiency (Blommaert et  
53 al., 2019; Matsuda-Lennikov et al., 2019).

54 Utilisation of potential glycosylation sites or sequons is not guaranteed and is dependent on the  
55 position within the chain (Nilsson and von Heijne, 2000; Ruiz-Canada et al., 2009; Shrimal et al.,  
56 2013), or the amino acid context of the site (Shrimal and Gilmore, 2013) with the kinetics of the  
57 folding or collapse of the polypeptide chain affecting glycosylation. Sequons buried within a protein  
58 structure, present at the amino or carboxy terminus or close to cysteines involved in disulfide  
59 formation may be underutilised giving rise to heterogeneity in glycoprotein forms.

60 Hypoglycosylation of sequons due to disulfide formation can be dependent upon STT3A or STT3B  
61 and is reversed when proteins are prevented from forming disulfides under highly reducing conditions  
62 (Allen et al., 1995; Cherepanova et al., 2014). In addition, STT3B-dependent glycosylation of  
63 cysteine-proximal sites requires the oxidoreductase activity of the thioredoxin-domain containing  
64 subunits MagT1 or TUSC3 (Cherepanova and Gilmore, 2016; Cherepanova et al., 2014). Structural  
65 analysis of TUSC3 indicates its direct binding to cysteine-containing peptides, suggesting direct  
66 binding to the polypeptide to slow down protein folding and disulfide formation to allow  
67 glycosylation to occur (Mohorko et al., 2014). The fact that MagT1 is mainly oxidised in cells  
68 (Cherepanova et al., 2014) would suggest that it acts as a reductase, thereby preventing disulfide

69 formation prior to glycosylation. Taken together these observations indicate a crucial role for the  
70 STT3B complex in coupling disulfide formation and glycosylation to maximise utilisation of  
71 cysteine-proximal acceptor sites.

72 The temporal relationship between disulfide formation and glycosylation suggests that the redox  
73 status of the ER may contribute towards sequon utilisation (Cherepanova et al., 2016). ER redox  
74 reactions are balanced to allow both disulfide formation and reduction resulting in the formation of  
75 the correct disulfides within folding proteins (Bulleid and van Lith, 2014). Members of the protein  
76 disulfide isomerase (PDI) family are thioredoxin-domain containing proteins that catalyse disulfide  
77 exchange reactions (Bulleid, 2012). Their oxidation is catalysed by Ero1, which couples the reduction  
78 of oxygen to the formation of a disulfide in PDI (Cabibbo et al., 2000). Specific members of the PDI  
79 family, such as ERp57 (Jessop et al., 2007) and ERdj5 (Oka et al., 2013; Ushioda et al., 2008)  
80 catalyse the reduction of non-native disulfides either allowing the correct disulfides to form or  
81 targeting misfolded proteins for degradation. Exactly how these PDI enzymes are reduced is  
82 unknown but recent evidence suggests a role for the cytosolic reductive pathway in correct disulfide  
83 formation, driven by the reduction of thioredoxin reductase (Cao et al., 2020; Poet et al., 2017).

84 It is likely that the ER oxidative and reductive pathways influence the STT3B subunits, MagT1 and  
85 TUSC3 during oxidoreductase activity towards cysteines proximal to sequons. Hence, the correct  
86 utilisation of sequons may well be regulated by the prevailing redox conditions within the ER. To  
87 address the role of ER redox conditions on utilisation of STT3B-dependent acceptor sites we  
88 capitalised on a recently described *in vitro* translation system that reproduces the early stages of  
89 secretory protein ER translocation and modification under defined redox conditions (Poet et al., 2017;  
90 Robinson and Bulleid, 2020). In this system, the redox conditions can be manipulated simply by the  
91 addition of glucose 6-phosphate (G6-P) which recycles NADPH thereby driving the cytosolic  
92 reductive pathway. When a source of ER is included during translation, the newly synthesised  
93 proteins are translocated across the ER membrane and can undergo both disulfide formation and N-  
94 linked glycosylation (Wilson et al., 1995). We chose to translate the STT3B-dependent substrate  
95 hemopexin (Cherepanova et al., 2014) in such a system, and show that it is hypoglycosylated in the  
96 absence of added G6-P, an effect that is reversed upon G6-P inclusion. Our results highlight the role  
97 of ER redox in the efficiency of sequon glycosylation and reveals an unexpected role for the NADPH-  
98 dependent cytosolic reductive pathway in the function of both the STTA and STT3B-containing OST  
99 complex.

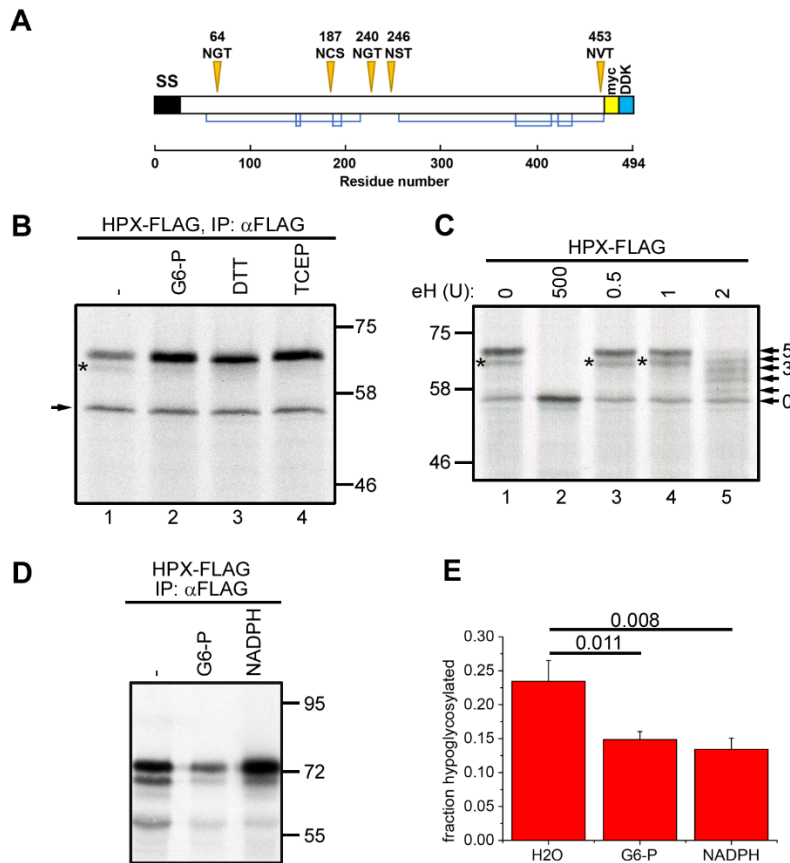
100 **Results**

101 **Cytosolic reductive pathway determines the extent of sequon usage in a STT3B-dependent**  
102 **glycoprotein.**

103 Our initial experiments aimed to determine whether the redox conditions within the ER had any effect  
104 on the fidelity of sequon usage within a model protein, hemopexin, that had previous been shown to  
105 undergo STT3B-dependent hypoglycosylation. Hemopexin has 5 potential sequons and forms six  
106 disulfides (Fig. 1A). For these experiments we adjusted the redox status of our *in vitro* translation  
107 reactions by adding specific components to the rabbit reticulocyte lysate. We have previously shown  
108 that a commercial reticulocyte lysate that has no added DTT allows disulfides to form in proteins  
109 synthesised even in the absence of semi-permeabilised (SP) cells as a source of ER (Poet et al., 2017).  
110 Supplementing this lysate with G6-P to drive G6-P dehydrogenase (G6PDH) and thioredoxin  
111 reductase (TrxR1) activity, renders this lysate sufficiently reducing to prevent disulfide formation in  
112 proteins synthesised without SP cells but allows disulfide formation in translocated proteins when SP-  
113 cells are present. When hemopexin was translated in the absence of added G6-P and presence of SP-  
114 cells we noted the appearance of two potential glycoforms giving rise to a doublet after SDS-PAGE  
115 (Fig. 1B, lane 1). We also see an additional product of approximately 55 kDa (indicated with an  
116 arrow) that most likely corresponds to untranslocated and, therefore, unglycosylated protein. When  
117 G6-P was added to the translation, the slower migrating glycoforms predominates (lane 2). Likewise,  
118 only the slower migrating glycoform was synthesised when translations were carried out in the  
119 presence of the membrane permeable and impermeable reducing agent DTT or TCEP respectively  
120 (lanes 3 and 4). Hence it would appear that hemopexin is hypoglycosylated in the absence of G6-P,  
121 an effect that is reversed when translations were carried out under more reducing conditions. As G6-P  
122 most likely alters the redox conditions by recycling NADP to NADPH in the cytosol and TCEP is  
123 membrane impermeable these results suggest that the redox conditions on the cytosolic side of the ER  
124 membrane are affecting the glycosylation efficiency of ER translocated hemopexin.

125 To verify that the two translation products seen after synthesis of hemopexin are indeed glycoproteins  
126 and to identify the status of the faster migrating band, we carried out a limited digestion of the protein  
127 with endoglycosidase (endo) H (Fig. 1C). Digestion of the translation products with the highest  
128 enzyme concentration resulted in a single band corresponding to the fully deglycosylated protein  
129 indicating that the two products are indeed glycoforms (lanes 1 and 2). Addition of limiting amounts  
130 of endo H to the reaction allowed partial digestion revealing all 5 potential glycoforms that arise from  
131 variable digestion of the five oligosaccharide side chains on hemopexin (lane 5). From this analysis  
132 we can conclude that the two apparent glycoforms seen when hemopexin is translated in the absence  
133 of added G6-P are indeed the 5 and 4 glycan forms. These results are consistent with our previously  
134 observed hypoglycosylation of hemopexin when expressed in mammalian cells (Shrimal and Gilmore,  
135 2013).

136 To verify that the reversal of hemopexin hypoglycosylation by G6-P is mediated by the recycling of  
 137 NADP, we supplemented the translation reactions with NADPH (Fig. 1D, E). As with G6-P, we  
 138 could reverse the hypoglycosylation of hemopexin just by adding NADPH confirming that the effect  
 139 is not due to G6-P directly influencing the glycosylation machinery or synthesis of the  
 140 oligosaccharide side chain.



141

142 **Figure 1. Hemopexin hypoglycosylation is prevented by G6-P or NADPH when included during**  
 143 **translation**

144 (A) Schematic diagram of hemopexin showing glycosylation sites (orange triangles), disulfide bond connectivity  
 145 (blue lines). The positions of the signal peptide (SS) and the myc- and DDK-tags are also indicated.

146 (B) Hemopexin was translated *in vitro* in the presence of SP cells in the absence or presence of 5 mM G6-P, 5  
 147 mM DTT or 1 mM TCEP for 1 hour. The SP cells were washed, lysed and hemopexin was immuno-isolated with  
 148 an anti-FLAG antibody, followed by separation by SDS-PAGE. The asterisk indicates hypoglycosylated  
 149 hemopexin, the arrow indicates non-translocated, non-glycosylated hemopexin.

150 (C) Hemopexin was translated as in (B) in the absence of G6-P. After lysis, the samples were incubated with  
 151 different amounts of endo H (indicated as units) at 37°C for 15 minutes and analysed by SDS-PAGE. The  
 152 asterisk indicates hypoglycosylated hemopexin, the arrows point to the different glycosylated species.

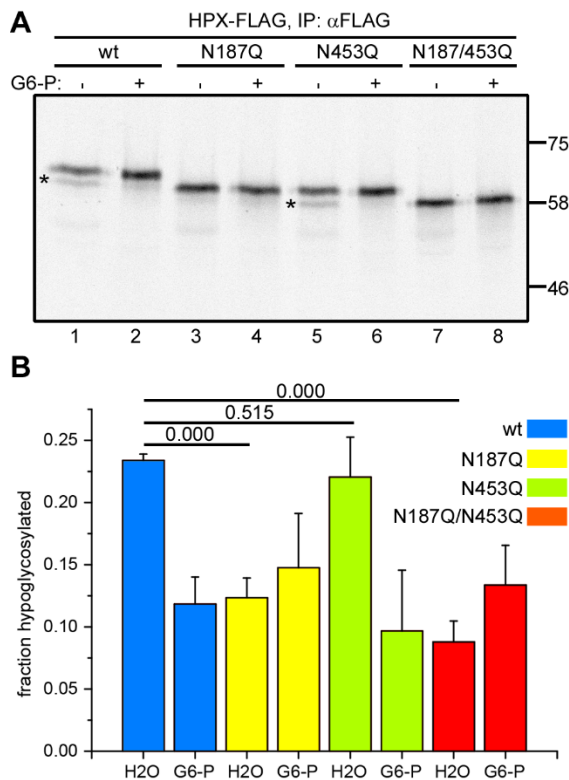
153 (D) Hemopexin was translated as in (B) in the absence or presence of 5 mM G6-P or 1 mM NADPH for 30  
 154 minutes. The translation reactions were analysed as in (B).

155 (E) Quantification of hemopexin hypoglycosylation of three independent experiments as in (D). Error bars are  
 156 standard deviation of mean. *p*-values of student's *t*-test are shown above the bar diagram.

### 157 Defining the sequon giving rise to G6-P-dependent hypoglycosylation

158 To determine which sequon within hemopexin is hypoglycosylated, we mutated hemopexin N187 and  
 159 N453 to glutamine, as it has been noted before that these sequons can frequently be skipped by the

160 oligosaccharyl transferases (Shrimal and Gilmore, 2013). We found that hypoglycosylation in the  
161 absence of G6-P occurred with wild type hemopexin and hemopexin N453Q, which can be resolved  
162 by the addition of G6-P (Fig. 2A, lanes 1, 2 and 5, 6). No hypoglycosylation was observed with  
163 hemopexin when N187 is mutated in either the single or double mutant (lanes 3 and 7).  
164 Quantification of the level of hypoglycosylation from three separate experiments supports the  
165 qualitative gel analysis (Fig. 2B). These results demonstrate that N187 is the acceptor site that is  
166 inefficiently glycosylated when translated in the presence of SP-cells and in the absence of added G6-  
167 P.



168

169 **Figure 2. Hemopexin hypoglycosylation occurs at sequon N187.**

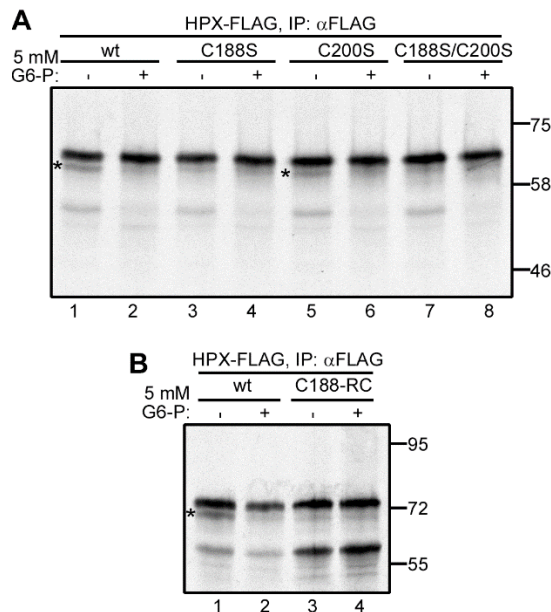
170 (A) Wild-type and N-glycosylation mutants of hemopexin were in vitro translated in the presence of SP cells in  
171 the absence or presence of 5 mM G6-P. The SP cells were washed, lysed and hemopexin was immuno-isolated  
172 followed by SDS-PAGE and autoradiography. Hypoglycosylated hemopexin is indicated by asterisks.

173 (B) Quantification of hemopexin hypoglycosylation of three independent experiments as in (A). Error bars are  
174 standard deviation of mean. p-values of student's t-test are shown above the bar diagram.

175 The N187 sequon is NCS with the C188 forming a short-range disulfide with C200 in the native  
176 structure of hemopexin (Fig. 1A) (Paoli et al., 1999). As it has been observed previously that  
177 cysteine-proximal glycosylation sites are often skipped (Cherepanova et al., 2014), we evaluated the  
178 role of hemopexin C188 in hypoglycosylation. In addition, to determine if the formation of the C188-  
179 C200 disulfide prevents efficient glycosylation, we mutated both cysteines individually and together  
180 to serine. We found that mutation of the more distal C200 did not prevent hypoglycosylation, which  
181 was resolved by inclusion of G6-P (Fig. 3A, lanes 5 and 6). In contrast, mutation of C188, in either



182 C188S or C188S/C200S mutant, resulted in almost complete loss of hypoglycosylation (lanes 3 and  
183 7).



184

### 185 **Figure 3. Disulfide formation via C188 results in hemopexin hypoglycosylation**

186 (A) Wild-type and cysteine mutants of hemopexin were translated *in vitro* in the presence of SP cells in the  
187 absence or presence of 5 mM G6-P for 1 hour. The SP cells were washed, lysed, immune-isolated and analysed  
188 by SDS-PAGE and autoradiography. Hypoglycosylated hemopexin is indicated by asterisks.

189 (B) Wild-type hemopexin and hemopexin lacking all mature protein cysteines except C188 were translated *in vitro*  
190 into SP cells in the absence or presence of 5 mM G6-P for 1 hour, and analysed as in (A).

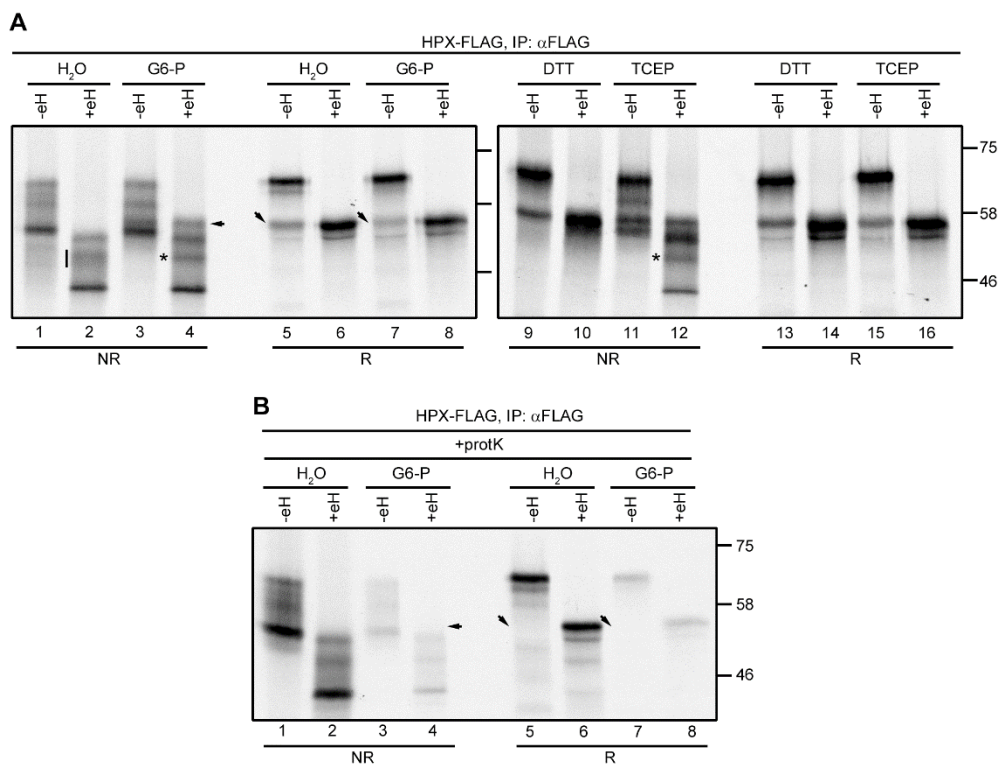
191 Preventing the native disulfide from forming by mutating C200 did not stop hypoglycosylation of the  
192 acceptor site whereas mutating C188 did, suggesting that the presence of the cysteine restricts  
193 glycosylation rather than the disulfide per se. Alternatively, C188 could be oxidised or form a non-  
194 native disulfide to an alternate cysteine to C200. To test these two possibilities, we created a  
195 construct where we mutated all the cysteines in the sequence apart from the cysteine at C188. Upon  
196 translation the protein was fully glycosylated either in the presence or absence of G6-P (Fig. 3B, lanes  
197 3 and 4). This result suggests that the formation of either a native or non-native disulfide via C188  
198 restricts the ability of the OST from glycosylating N187 resulting in hypoglycosylation. In addition, it  
199 shows that it is a change in the redox conditions during synthesis that is reversed by the inclusion of  
200 G6-P maintaining the C188 in a reduced state to allow efficient glycosylation.

### 201 **Hemopexin forms distinct disulfide-bonded species during translation in the absence or** 202 **presence of added G6-P**

203 The ability of C188 to form a native or non-native disulfide affected N187 occupancy, which suggests  
204 a role for G6-P in modulating disulfide formation in our translation system. Indeed, we have  
205 previously shown that addition of G6-P prevents non-native disulfide formation in a variety of  
206 proteins by recycling NADPH and maintaining cytosolic thioredoxin in a reduced state (Poet et al.,  
207 2017). To determine the redox status of hemopexin following translation, we prevented disulfide



208 rearrangement following synthesis using an alkylating agent and separated the translation products  
209 under non-reducing conditions. Typically, long-range disulfides formed in proteins affect their  
210 electrophoretic mobility by altering the hydrodynamic volume of the denatured protein. When the  
211 hemopexin translation products were analysed this way, we observed several oxidised species with a  
212 greater mobility than the reduced protein (Fig. 4A, compare lane 1 and 5). To rule out any  
213 contribution of hypoglycosylation to the pattern under non-reducing conditions, the samples were also  
214 treated with endo H to remove all glycans (even numbered lanes). Multiple oxidised species were still  
215 observed indicating that hemopexin forms distinct and incompletely disulfide-bonded species in our  
216 translation system.



217

218 **Figure 4. Hemopexin forms several disulfide-bonded species when translated in the presence or**  
219 **absence of G6-P**

220 (A) Hemopexin was translated *in vitro* in the presence of SP cells in the absence or presence of 5 mM G6-P, 5  
221 mM DTT or 1 mM TCEP. The translations were stopped by adding 20 mM N-ethyl maleimide and incubation  
222 on ice. After lysis, the samples were mock treated or treated with endo H, followed by immuno-isolation and  
223 analysis by reducing (R) and non-reducing (NR) SDS-PAGE. The vertical line and asterisks indicate a change  
224 in oxidation state when *in vitro* translations were carried in the presence of G6-P or TCEP.

225 (B) Hemopexin was translated as in (A). After the addition of 20 mM NEM and pelleting the SP cells, the cells  
226 were treated with proteinase K, followed by lysis and endo H treatment. The samples were immuno-isolated and  
227 analysed by reducing (R) and non-reducing (NR) SDS-PAGE. The arrows in (A) and (B) point to bands that  
228 disappear upon proteinase K treatment.

229 When the translations were carried out in the presence of G6-P, most of the oxidised species migrated  
230 as those in untreated lysates (lane 1 and 2 vs 3 and 4). One species appeared after G6-P addition, seen  
231 in the endoH treated samples (lane 2 versus 4, indicated by an arrow). This translation product was  
232 digested by proteinase K, indicating that it corresponds to untranslocated hemopexin (Fig. 4B, lane 4,

233 arrow). The removal of untranslocated material is most clearly seen when the samples are separated  
234 under reducing conditions (lane 5 and 7, down arrows). The remainder of the bands are protected  
235 from proteinase K digestion, indicated that all these species are translocated into the ER lumen. The  
236 dramatic change to the redox status of untranslocated protein is consistent with our previous studies  
237 indicating that the addition of G6-P restores a robust reducing pathway in the cytosol, but does not  
238 prevent correct disulfide formation in proteins translocated across the ER membrane (Poet et al.,  
239 2017; Robinson and Bulleid, 2020). Interestingly, the oxidised species migrating with intermediate  
240 mobility become less diffuse after G6-P addition (lanes 2 and 4, vertical line and asterisk) suggesting  
241 some rearrangement of disulfides.

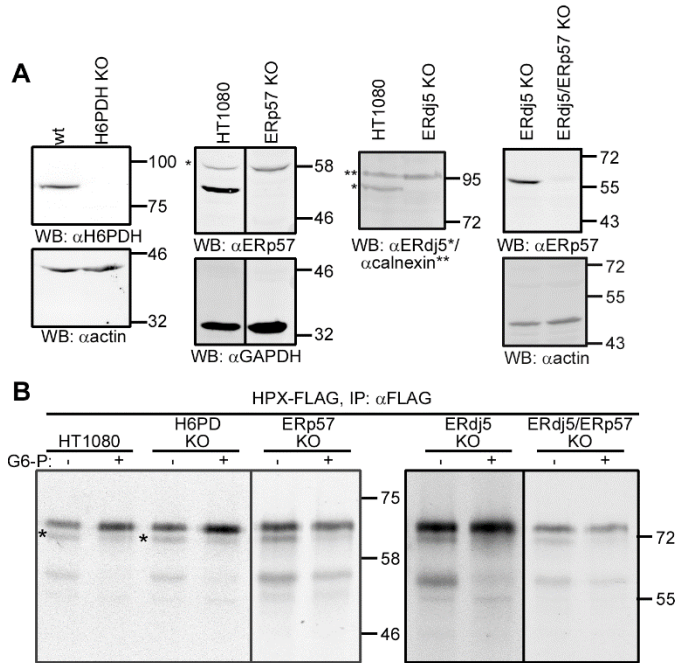
242 Adding the reductant DTT to the hemopexin *in vitro* translations prevented disulfide formation  
243 resulting in a non-reducing pattern that resembled that of the samples run under reducing conditions  
244 (Fig. 4A, lanes 9 and 10 vs 13 and 14). In contrast, the addition of the membrane impermeable  
245 reductant TCEP to the reactions gave a non-reducing pattern like that following G6-P addition (lanes  
246 3 and 4 versus 11 and 12), including the sharpening of the intermediate oxidised species (lane 12,  
247 asterisk). Both the addition of TCEP and G6-P altered the overall pattern of translocated disulfide-  
248 bonded forms and TCEP and to some extent G6-P addition resulted in a shift in their ratios with more  
249 of the slower migrating form present following their addition (compare lanes 2, 4 and 12). Hence,  
250 G6-P inclusion caused subtle but distinct differences in the oxidised species present indicative of  
251 rearrangement of non-native disulfides. While the addition of G6-P, TCEP or DTT had different  
252 effects on the redox species formed, they all resulted in full hemopexin glycosylation.

### 253 **G6-P does not act via an ER NADPH pool or PDIs involved in non-native disulfide reduction**

254 The results presented so far would suggest a requirement to maintain a robust cytosolic reductive  
255 pathway to ensure the efficient glycosylation of hemopexin. Alternatively, G6-P can be transported  
256 into the lumen of the ER by the glucose-6-phosphate transporter (G6PT), where it can be used by the  
257 ER-localised hexose-6-phosphate dehydrogenase (H6PDH) to locally generate NADPH (Clarke and  
258 Mason, 2003). The NADPH could be used to provide reducing equivalents for the promotion of  
259 hemopexin glycosylation by a yet unidentified pathway. To determine if the ER NADPH pool is  
260 involved, we evaluated the effect of G6-P on hemopexin glycosylation using SP-cells derived from a  
261 H6PDH knock out (KO) cell-line (Fig. 5A). G6-P addition still reversed the hypoglycosylation of  
262 hemopexin in this cell line ruling out a role for H6PDH (Fig. 5B).

263 The fact that hypoglycosylation of hemopexin can be influenced by a disulfide formed via C188 led  
264 us to determine whether previously characterised PDIs that have reductase activity might be involved  
265 directly or via disulfide exchange with the STT3B-subunits MagT1 or TUSC3. We focused on the  
266 PDIs ERp57 and ERdj5 as they are known to catalyse the reduction of non-native disulfides (Jessop et  
267 al., 2007; Oka et al., 2013; Ushioda et al., 2008). We created KO cell-lines for the individual proteins

268 as well as a combined ERdj5-ERp57 double KO (Fig. 5A). For each of these cell-lines there was no  
 269 effect on the reversal of hypoglycosylation facilitated by G6-P (Fig. 5B). Hence the reductive  
 270 pathway maintained by the addition of G6-P functions independently from the known ER PDI  
 271 reductases.



272

273 **Figure 5. ERp57, ERdj5 or H6PDH are not required for efficient hemopexin glycosylation**

274 (A) Western blot analysis for H6PDH, ERp57, ERdj5 and ERp57+ERdj5 knockout cell lines showing lack of  
 275 expression for each knocked-out protein. Actin, GAPDH and calnexin are used as loading controls.

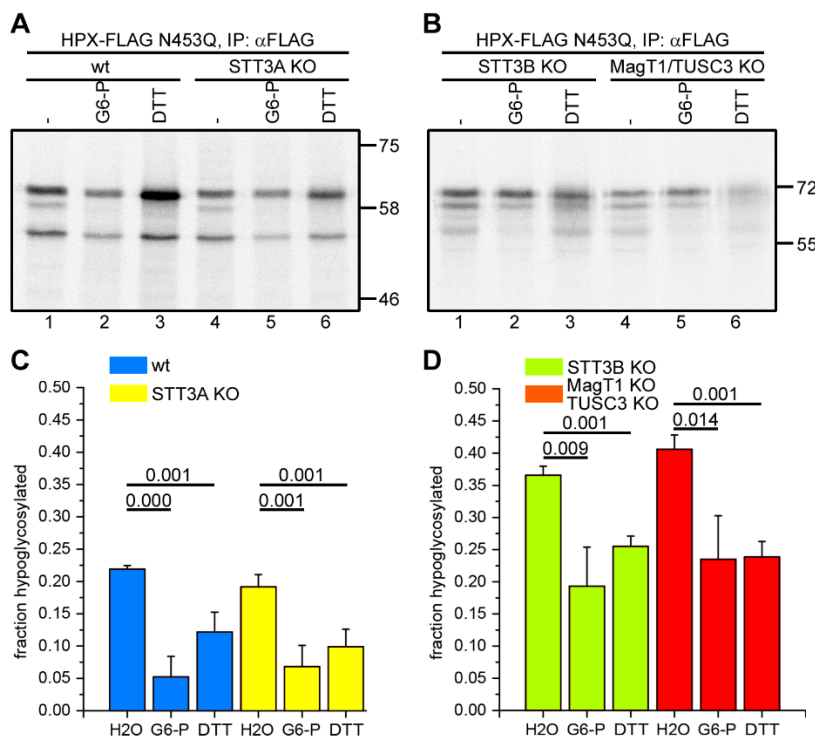
276 (B) Hemopexin was *in vitro* translated in the presence of SP cells derived from H6PDH, ERp57, ERdj5 or  
 277 ERp57+ERdj5 knockout cell lines in the absence or presence of 5 mM G6-P for 1 hour. The *in vitro* translations  
 278 were analysed as in Fig. 3.

279 **Role of the OST complexes containing either STT3A or STT3B catalytic subunits.**

280 To determine whether STT3A or STT3B are required for the G6-P effect on hemopexin glycosylation,  
 281 we used two previously characterised KO cell lines for STT3A and STT3B (Cherepanova and  
 282 Gilmore, 2016). To look specifically at glycosylation of the cysteine proximal N187 we used the  
 283 hemopexin N453Q mutant for *in vitro* translation in SP cells derived from these KO cell lines.  
 284 Previously, the N453 site had been shown to be STT3B-dependent (Shrimal and Gilmore, 2013).  
 285 Hemopexin N453Q translated into STT3A KO SP cells was glycosylated similarly to that in wild type  
 286 cells, with both G6-P and DTT able to partially resolve the hypoglycosylation (Fig. 6A, lanes 4-6  
 287 versus 1-3 and Fig. 6C). These results indicate that the effect of G6-P seen in wild type cells is not  
 288 due to the STT3A OST.

289 In contrast, hemopexin hypoglycosylation is more pronounced in STT3B KO cells in the absence of  
 290 G6-P with levels of 35-40% hypoglycosylation as compared with 20-25% in wild type cells (Fig. 6B  
 291 and D compared to Fig. 6A). There was an effect of adding G6-P or DTT which reduced the  
 292 hypoglycosylation to wild-type levels seen in the absence of reducing agent (Fig. 6D). In STT3B

293 knockout cells, not only is the STT3B catalytic activity abolished, but these cells have also lost  
 294 expression of the STT3B-specific subunits MagT1/TUSC3 (Cherepanova and Gilmore, 2016). To see  
 295 if there is a direct contribution of MagT1/TUSC3, we used SP cells derived from MagT1/TUSC3 KO  
 296 cells for *in vitro* translation of hemopexin. Like with the STT3B KO cells, hemopexin  
 297 hypoglycosylation was more pronounced in the absence of G6-P and, when either G6-P or DTT was  
 298 included during translation, hypoglycosylation was reduced to the levels seen in wild type cells in the  
 299 absence of G6-P (Fig. 6B, lanes 4-6 and Fig. 6D). Thus, efficient glycosylation of hemopexin N187  
 300 is dependent on the STT3B complex and specifically the TUSC3 or MagT1 subunits.



301

302 **Figure 6. STT3A and STT3B dependence on hemopexin glycosylation.**

303 (A)(B) Hemopexin N453Q was translated *in vitro* in the presence of SP cells derived from wild-type, STT3A,  
 304 STT3B or MagT1/TUSC3 KO cells in the absence or presence of 5 mM G6-P or 5 mM DTT at 30°C for 1 hour.  
 305 After immuno-isolation, hemopexin was analysed by SDS-PAGE.

306 (C)(D) Quantification of hypoglycosylated hemopexin of 4 and 3 independent experiments for (A) and (B),  
 307 respectively. Error bars are standard deviation of mean. *p*-values of student's *t*-test are shown above the bar  
 308 diagram.

309

## 310 Discussion

311 Previous work demonstrated a role for the STT3B-associated oxidoreductase subunits MagT1 or  
312 TUSC3 in ensuring the efficient glycosylation of the STT3B-dependent substrate hemopexin  
313 (Cherepanova et al., 2014). Here we extend this work to demonstrate that the redox conditions within  
314 the ER contribute towards sequon utilisation and that the cytosolic reductive pathway plays a key role  
315 in maintaining the optimal redox balance for STT3B activity. We find that the efficiency of cysteine-  
316 proximal acceptor site usage is likely dependent upon the timing of disulfide formation. If a disulfide  
317 forms prior to glycosylation by the STT3A containing OST, the site may be skipped and requires a  
318 STT3B dependent reduction of the disulfide to allow glycosylation. In addition, the function of  
319 STT3B containing OST is dependent upon the thioredoxin-like subunits MagT1 or TUSC3 and their  
320 activity in reducing any disulfides requires a robust reductive pathway. Hence, the cytosolic reductive  
321 pathway influences the initial glycosylation by STT3A by delaying disulfide formation as well as  
322 optimising STT3B function in glycosylation of sites missed by STT3A due to rapid disulfide  
323 formation. The cytosolic reductive pathway is itself dependent upon the presence of an active pentose  
324 phosphate pathway to ensure the recycling of NADPH illustrating a connection between cellular  
325 metabolism and glycosylation efficiency. While such a link has been suggested previously  
326 (Gansemer et al., 2020), our observations provide a previously unappreciated correlation between  
327 cellular metabolism and the variability in synthesis of protein glycoforms.

328 If the ability of STT3A to glycosylate the N187 sequon is determined by whether a disulfide has  
329 formed, this would indicate that the STT3B containing OST needs to first reduce any disulfide  
330 between C188 and C200 prior to glycosylating this site. Hence, the MagT1 or TUSC3 subunits would  
331 act as reductases which is suggested by the relatively low reduction potential of its active site thiols  
332 and by the fact that it is predominantly in an oxidised form in the ER (Cherepanova et al., 2014;  
333 Mohorko et al., 2014). In addition, substrate trapping mutants of MagT1, where the second cysteine  
334 in the CXXC active site was mutated to serine, form mixed disulfides to substrate proteins, further  
335 confirming the ability to act as a reductase (Cherepanova et al., 2014). For the enzyme to function as  
336 a reductase its active site must be reduced either by a low molecular weight thiol such as glutathione  
337 or by disulfide exchange with another protein. The reduction potential of glutathione is higher than  
338 MagT1 (Mohorko et al., 2014) so it would be a thermodynamically unfavourable reaction, but cannot  
339 be ruled out due to the high cellular glutathione concentration (Jensen et al., 2009). Strong candidates  
340 for disulfide exchange reactions would be members of the ER-localised PDI family, though two of the  
341 previously characterised reductases ERp57 and ERdj5 do not appear to influence the G6-P dependent  
342 hypoglycosylation of hemopexin. Due to the large repertoire of PDI family members (Hatahet and  
343 Ruddock, 2007), it is likely that there is redundancy in their ability to facilitate disulfide exchange  
344 making the identification of reductases for MagT1 or TUSC3 challenging.

345 The transfer of reducing equivalents across the ER membrane is most likely brought about by a  
346 transmembrane protein (Cao et al., 2020), which could directly or indirectly reduce MagT1 or  
347 TUSC3. The requirement for such a conduit for reducing equivalents has been demonstrated to allow  
348 native disulfides to form in proteins entering the secretory pathway (Poet et al., 2017). Here, the  
349 presence of such a transmembrane protein is suggested by the ability of added NADPH to reverse  
350 hypoglycosylation and the fact that the ER membrane is essentially non-permeant to either NADP or  
351 NADPH (Piccirella et al., 2006). This fact, combined with the lack of a role for the ER-localised  
352 H6PDH, would suggest an indirect effect on ER redox status facilitated by the transfer of reducing  
353 equivalents across the ER membrane. In addition, the ability to reverse hypoglycosylation with the  
354 membrane impermeable reducing agent TCEP suggests an indirect effect on OST function. Whether  
355 the same membrane components are required to ensure the fidelity of disulfide formation and STT3B  
356 containing OST function remains to be determined.

357



## 358 **Materials and Methods**

### 359 *Cell lines, constructs, and reagents*

360 The HT1080 and 293 HEK cell lines were cultured in DMEM (Gibco) supplemented with 2 mM  
361 glutamine, 100 U/ml penicillin, 100 µg/ml streptomycin and 10% foetal calf serum (Sigma). The  
362 wild-type, STT3A, STT3B and MagT1/TUSC3 293 HEK knockout cell lines were created as  
363 described (Cherepanova and Gilmore, 2016). The antibodies against FLAG-tag (Sigma F3165),  
364 H6PDH (Abcam ab119046), actin (Sigma A2103), DNAJC10 (ERdj5) (Abnova, H00054431-M01A)  
365 and GAPDH (Ambion AM4300) were obtained commercially. The antibody to ERp57 was raised as  
366 described (Jessop and Bulleid, 2004). Myc- and DDK-tagged hemopexin plasmid was purchased  
367 from Origene. Glycosylation and cysteine mutations were made with the Quick Change II Site-  
368 Directed Mutagenesis kit (Promega). A synthetic construct coding for the hemopexin sequence  
369 without any cysteines apart from cys188 was purchased from Genescript. Glucose-6-phosphate, N-  
370 ethylmaleimide and DTT were obtained from Sigma. Tris(2-carboxyethyl) phosphine (TCEP) was  
371 purchased from Thermo Fisher.

### 372 *In vitro* transcription and *in vitro* translation

373 Myc- and DDK (FLAG)-tagged Hemopexin mRNA was transcribed from an AgeI (NEB) linearised  
374 plasmid using T7 RNA polymerase (Promega). *In vitro* translation (Poet et al., 2017) and preparation  
375 of semi-permeabilised (SP) cells (Wilson et al., 1995) was carried out as described previously.  
376 Briefly, the mRNA was translated in a Flexi rabbit reticulocyte lysate (Promega) containing <sup>35</sup>S  
377 methionine/cysteine (Perkin Elmer) in the presence of SP-cells at 30°C for 1 hour. Where indicated  
378 the translation reaction was supplemented with G6-P (5 mM), DTT (5 mM), TCEP (1 mM) or  
379 NADPH (1 mM). The SP cells were pelleted by centrifugation and washed with KHM buffer (110  
380 mM KAc, 2 mM MgAc, 20 mM Hepes pH 7.2) followed by lysis, preclearing with agarose beads and  
381 immunoprecipitation with anti-FLAG antibody and protein G beads (Generon). The samples were  
382 analysed by SDS-PAGE and visualised by exposure to film (Kodak) or phosphorimager plates  
383 (Fujifilm FLA-7000). Quantifications were performed with ImageJ (<https://imagej.nih.gov/ij/>) using  
384 phosphorimager scans and were calculated as the fraction that is hypoglycosylated  
385 (hypo/(hypo+full)).

386 To distinguish between translocated and non-translocated translation products, after translations the  
387 SP cells were incubated on ice with 10 µg/ml proteinase K (Roche) in the presence of 1 mM CaCl<sub>2</sub> for  
388 25 minutes. The digestion was stopped with 0.5 mM PMSF before further analysis. Where indicated,  
389 the lysates were treated with endoglycosidase H (NEB).

### 390 *CRISPR-Cas 9 knockout cell-lines*

391 Hexose-6-phosphate dehydrogenase (H6PDH) knockout cells were created by CRISPR-Cas9, using a  
392 two-guide (GGATTATGGAGACATGTCCC and GCCATAAGTACTTCTTAGCC) Cas9 D10A  
393 nickase system (Kabadi et al., 2014). The same system was used for the creation of the ERp57 KO  
394 cells using the guide sequences (TTCTAGCACGTCGGAGGCAG and  
395 CGAGAGTCGCATCTCCGACA). The ERdj5 knockout cells were created using the Integrated  
396 DNA Technologies (IDT) Alt-R CRISPR-Cas 9 System, the predesigned gRNA to knock out ERdj5  
397 (GTGTATATGGCCATTTTAGT) was selected. We used a single gRNA (crRNA) duplexed with a  
398 tracrRNA (IDT, 1072532) and Alt-R S.p. HiFi Cas9 Nuclease V3 (IDT, 1081060) for genome editing.  
399 To generate an ERp57 knockout, Cas9 nuclease was added to a duplex of 1AB crRNA:tracrRNA in  
400 Optimem to form the RNP complex (Fisher, 31985062), which was then transfected into HT1080  
401 cells using Lipofectamine CRISPRMAX transfection reagent (Thermo Fisher). Cells were transferred  
402 to 15 cm dishes until colonies appeared (about 10-12 days later). All positive knockout cells were  
403 identified by western blotting using either anti-DNAJC10 (ERdj5), anti-H6PDH or anti-ERp57 and  
404 deletion verified by sequencing. The ERp57/ERdj5 knockout cell-line was created from the ERdj5  
405 KO cells using the Alt-R CRISPR-Cas 9 system, with the ERp57 gRNA  
406 (GTCCGTGAGTTCTAGCACGT) (IDT).

407 **References**

- 408 **Allen, S., Naim, H. Y. and Bulleid, N. J.** (1995). Intracellular folding of tissue-type  
409 plasminogen activator. Effects of disulfide bond formation on N-linked glycosylation and secretion. *J*  
410 *Biol Chem* **270**, 4797-804.
- 411 **Blomen, V. A., Majek, P., Jae, L. T., Bigenzahn, J. W., Nieuwenhuis, J., Staring, J.,**  
412 **Sacco, R., van Diemen, F. R., Olk, N., Stukalov, A. et al.** (2015). Gene essentiality and synthetic  
413 lethality in haploid human cells. *Science* **350**, 1092-6.
- 414 **Blommaert, E., Peanne, R., Cherepanova, N. A., Rymen, D., Staels, F., Jaeken, J., Race,**  
415 **V., Keldermans, L., Souche, E., Corveleyn, A. et al.** (2019). Mutations in MAGT1 lead to a  
416 glycosylation disorder with a variable phenotype. *Proc Natl Acad Sci U S A* **116**, 9865-9870.
- 417 **Braunger, K., Pfeffer, S., Shrimal, S., Gilmore, R., Berninghausen, O., Mandon, E. C.,**  
418 **Becker, T., Forster, F. and Beckmann, R.** (2018). Structural basis for coupling protein transport and  
419 N-glycosylation at the mammalian endoplasmic reticulum. *Science* **360**, 215-219.
- 420 **Bulleid, N. J.** (2012). Disulfide bond formation in the mammalian endoplasmic reticulum.  
421 *Cold Spring Harb Perspect Biol* **4**.
- 422 **Bulleid, N. J. and van Lith, M.** (2014). Redox regulation in the endoplasmic reticulum.  
423 *Biochem Soc Trans* **42**, 905-8.
- 424 **Cabibbo, A., Pagani, M., Fabbri, M., Rocchi, M., Farmery, M. R., Bulleid, N. J. and**  
425 **Sitia, R.** (2000). ERO1-L, a human protein that favors disulfide bond formation in the endoplasmic  
426 reticulum. *J Biol Chem* **275**, 4827-33.
- 427 **Cao, X., Lilla, S., Cao, Z., Pringle, M. A., Oka, O. B. V., Robinson, P. J., Szmaja, T., van**  
428 **Lith, M., Zanivan, S. and Bulleid, N. J.** (2020). The mammalian cytosolic thioredoxin reductase  
429 pathway acts via a membrane protein to reduce ER-localised proteins. *J Cell Sci* **133**.
- 430 **Cherepanova, N., Shrimal, S. and Gilmore, R.** (2016). N-linked glycosylation and  
431 homeostasis of the endoplasmic reticulum. *Curr Opin Cell Biol* **41**, 57-65.
- 432 **Cherepanova, N. A. and Gilmore, R.** (2016). Mammalian cells lacking either the  
433 cotranslational or posttranslocational oligosaccharyltransferase complex display substrate-dependent  
434 defects in asparagine linked glycosylation. *Sci Rep* **6**, 20946.
- 435 **Cherepanova, N. A., Shrimal, S. and Gilmore, R.** (2014). Oxidoreductase activity is  
436 necessary for N-glycosylation of cysteine-proximal acceptor sites in glycoproteins. *J Cell Biol* **206**,  
437 525-39.
- 438 **Cherepanova, N. A., Venev, S. V., Leszyk, J. D., Shaffer, S. A. and Gilmore, R.** (2019).  
439 Quantitative glycoproteomics reveals new classes of STT3A- and STT3B-dependent N-glycosylation  
440 sites. *J Cell Biol* **218**, 2782-2796.
- 441 **Clarke, J. L. and Mason, P. J.** (2003). Murine hexose-6-phosphate dehydrogenase: a  
442 bifunctional enzyme with broad substrate specificity and 6-phosphogluconolactonase activity. *Arch*  
443 *Biochem Biophys* **415**, 229-34.
- 444 **Gansemer, E. R., McCommis, K. S., Martino, M., King-McAlpin, A. Q., Potthoff, M. J.,**  
445 **Finck, B. N., Taylor, E. B. and Rutkowski, D. T.** (2020). NADPH and Glutathione Redox Link  
446 TCA Cycle Activity to Endoplasmic Reticulum Homeostasis. *iScience* **23**, 101116.
- 447 **Hatahet, F. and Ruddock, L. W.** (2007). Substrate recognition by the protein disulfide  
448 isomerases. *FEBS J* **274**, 5223-34.
- 449 **Jensen, K. S., Hansen, R. E. and Winther, J. R.** (2009). Kinetic and thermodynamic aspects  
450 of cellular thiol-disulfide redox regulation. *Antioxid Redox Signal* **11**, 1047-58.
- 451 **Jessop, C. E. and Bulleid, N. J.** (2004). Glutathione directly reduces an oxidoreductase in  
452 the endoplasmic reticulum of mammalian cells. *J Biol Chem* **279**, 55341-7.
- 453 **Jessop, C. E., Chakravarthi, S., Garbi, N., Hammerling, G. J., Lovell, S. and Bulleid, N.**  
454 **J.** (2007). ERp57 is essential for efficient folding of glycoproteins sharing common structural  
455 domains. *EMBO J* **26**, 28-40.
- 456 **Kabadi, A. M., Ousterout, D. G., Hilton, I. B. and Gersbach, C. A.** (2014). Multiplex  
457 CRISPR/Cas9-based genome engineering from a single lentiviral vector. *Nucleic Acids Res* **42**, e147.
- 458 **Kelleher, D. J., Karaoglu, D., Mandon, E. C. and Gilmore, R.** (2003).  
459 Oligosaccharyltransferase isoforms that contain different catalytic STT3 subunits have distinct  
460 enzymatic properties. *Mol Cell* **12**, 101-11.

- 461 **Matsuda-Lennikov, M., Biancalana, M., Zou, J., Ravell, J. C., Zheng, L., Kanellopoulou,**  
462 **C., Jiang, P., Notarangelo, G., Jing, H., Masutani, E. et al.** (2019). Magnesium transporter 1  
463 (MAGT1) deficiency causes selective defects in N-linked glycosylation and expression of immune-  
464 response genes. *J Biol Chem* **294**, 13638-13656.
- 465 **Mohorko, E., Owen, R. L., Malojcic, G., Brozzo, M. S., Aebi, M. and Glockshuber, R.**  
466 (2014). Structural basis of substrate specificity of human oligosaccharyl transferase subunit  
467 N33/Tusc3 and its role in regulating protein N-glycosylation. *Structure* **22**, 590-601.
- 468 **Nilsson, I. and von Heijne, G.** (2000). Glycosylation efficiency of Asn-Xaa-Thr sequons  
469 depends both on the distance from the C terminus and on the presence of a downstream  
470 transmembrane segment. *J Biol Chem* **275**, 17338-43.
- 471 **Oka, O. B., Pringle, M. A., Schopp, I. M., Braakman, I. and Bulleid, N. J.** (2013). ERdj5  
472 is the ER reductase that catalyzes the removal of non-native disulfides and correct folding of the LDL  
473 receptor. *Mol Cell* **50**, 793-804.
- 474 **Paoli, M., Anderson, B. F., Baker, H. M., Morgan, W. T., Smith, A. and Baker, E. N.**  
475 (1999). Crystal structure of hemopexin reveals a novel high-affinity heme site formed between two  
476 beta-propeller domains. *Nat Struct Biol* **6**, 926-31.
- 477 **Piccirella, S., Czeglé, I., Lizak, B., Margittai, E., Senesi, S., Papp, E., Csala, M., Fulceri,**  
478 **R., Csermely, P., Mandl, J. et al.** (2006). Uncoupled redox systems in the lumen of the endoplasmic  
479 reticulum. Pyridine nucleotides stay reduced in an oxidative environment. *J Biol Chem* **281**, 4671-7.
- 480 **Poet, G. J., Oka, O. B., van Lith, M., Cao, Z., Robinson, P. J., Pringle, M. A., Arner, E.**  
481 **S. and Bulleid, N. J.** (2017). Cytosolic thioredoxin reductase 1 is required for correct disulfide  
482 formation in the ER. *EMBO J* **36**, 693-702.
- 483 **Robinson, P. J. and Bulleid, N. J.** (2020). Mechanisms of Disulfide Bond Formation in  
484 Nascent Polypeptides Entering the Secretory Pathway. *Cells* **9**.
- 485 **Roboti, P. and High, S.** (2012). The oligosaccharyltransferase subunits OST48, DAD1 and  
486 KCP2 function as ubiquitous and selective modulators of mammalian N-glycosylation. *J Cell Sci* **125**,  
487 3474-84.
- 488 **Ruiz-Canada, C., Kelleher, D. J. and Gilmore, R.** (2009). Cotranslational and  
489 posttranslational N-glycosylation of polypeptides by distinct mammalian OST isoforms. *Cell* **136**,  
490 272-83.
- 491 **Shibatani, T., David, L. L., McCormack, A. L., Frueh, K. and Skach, W. R.** (2005).  
492 Proteomic analysis of mammalian oligosaccharyltransferase reveals multiple subcomplexes that  
493 contain Sec61, TRAP, and two potential new subunits. *Biochemistry* **44**, 5982-92.
- 494 **Shrimal, S. and Gilmore, R.** (2013). Glycosylation of closely spaced acceptor sites in human  
495 glycoproteins. *J Cell Sci* **126**, 5513-23.
- 496 **Shrimal, S., Trueman, S. F. and Gilmore, R.** (2013). Extreme C-terminal sites are  
497 posttranslocationally glycosylated by the STT3B isoform of the OST. *J Cell Biol* **201**, 81-95.
- 498 **Ushioda, R., Hoseki, J., Araki, K., Jansen, G., Thomas, D. Y. and Nagata, K.** (2008).  
499 ERdj5 is required as a disulfide reductase for degradation of misfolded proteins in the ER. *Science*  
500 **321**, 569-72.
- 501 **Wilson, R., Allen, A. J., Oliver, J., Brookman, J. L., High, S. and Bulleid, N. J.** (1995).  
502 The translocation, folding, assembly and redox-dependent degradation of secretory and membrane  
503 proteins in semi-permeabilized mammalian cells. *Biochem J* **307 ( Pt 3)**, 679-87.

505 **Acknowledgements**

506 This work was funded by the Wellcome Trust (grant number 103720) and Medical Research Scotland  
507 (grant number: VAC-1417-2019).

508 **Author contributions**

509 The work described in this manuscript was conceived and supervised by NJB with contribution from  
510 MvL, and RG. The experimental work was carried out by MvL, MAP, BF, GG and JI. The data was  
511 analysed by MvL and NJB. The manuscript was written by NJB and MvL with editing by RG.

512 **Conflict of interest**

513 The authors declare that they have no conflict of interest.